Since January 2020 Elsevier has created a COVID-19 resource centre with free information in English and Mandarin on the novel coronavirus COVID-19. The COVID-19 resource centre is hosted on Elsevier Connect, the company's public news and information website.

Virology **298,** 258–270 (2002)
doi:10.1006/viro.2002.1495

Functional Properties of the Predicted Helicase of Porcine Reproductive and Respiratory Syndrome Virus

Elida M. Bautista,*[1] Kay S. Faaberg,† Dan Mickelson,† and Edward D. McGruder*

*Elanco Animal Health Research and Development, a Division of Eli Lilly and Company, P.O. Box 708, Greenfield, Indiana 64140; and †University of Minnesota, Department of Veterinary PathoBiology, 1971 Commonwealth Avenue, Saint Paul, Minnesota 55108

Received July 18, 2001; returned to author for revision September 17, 2002; accepted March 30, 2002

Porcine reproductive and respiratory syndrome virus (PRRSV) is a member of the positive-strand RNA virus family *Arteriviridae.* Although considerable research has focused on this important pathogen, little is known about the function of most PRRSV proteins. To examine characteristics of putative nonstructural proteins (nsp) encoded in ORF1b, which have been identified by nucleotide similarity to domains of equine arteritis virus, defined genomic regions were cloned and expressed in the pRSET expression system. One region, nsp10, encoded a protein with a putative helicase domain and was further examined for functional helicase-like activities. PRRSV nsp10 was found to possess a thermolabile and pH-sensitive NTPase activity that was modulated by polynucleotides and to unwind dsRNA in a 5′ to 3′ polarity. These results provide the first evidence of the functional properties of PRRSV helicase and further support the finding that nidovirus helicases possess properties that distinguish them from other viral helicases.

Key Words: PRRSV; arterivirus; coronavirus; *Nidovirales;* RNA-dependent RNA polymerase; helicase; NTPase.

INTRODUCTION

Porcine reproductive and respiratory syndrome virus (PRRSV) emerged in the late 1980s and became a pathogen of scientific interest due to its economic importance. Analysis of PRRSV structure, genomic organization, and expression and its biological, physicochemical, and pathogenic properties has shown that PRRSV is related to equine arteritis virus (EAV), lactate dehydrogenase-elevating virus of mice (LDV), and simian hemorrhagic fever virus (SHFV) (Benfield *et al.,* 1992; Collins *et al.,* 1992; Meulenberg *et al.,* 1993; Plagemann and Moennig, 1992). These viruses are grouped in a new family designated *Arteriviridae* and placed with the *Coronaviridae* family within the order *Nidovirales* (Cavanagh, 1997). PRRSV has been revealed to consist of two distantly related genotypes, North American (NA, 15.4 kb) and European (EU, 15.1 kb), based on sequence analysis (Allende *et al.,* 1999; Meulenberg *et al.,* 1993; Murtaugh *et al.,* 1995, 1998; Nelsen *et al.,* 1999). The genome of PRRSV encodes at least eight open reading frames (ORFs) that are expressed in the infected cell as a nested set of subgenomic mRNAs. ORF1, translated from the full-length RNA template, codes for replicase-related nonstructural proteins and is the focus of this study. ORFs 2 to 7 encode mostly structural polypeptides.

[1] To whom correspondence and reprint requests should be addressed at United States Department of Agriculture, Plum Island Animal Disease Center, P.O. Box 848, Greenport, NY 11944-0848. Fax: 631-323-3295. E-mail: Ebautista@piadc.ars.usda.gov.

ORF1 contains two long open reading frames, designated ORF1a and ORF1b, that are autocatalytically processed by virally encoded proteases (Meulenberg *et al.,* 1993). ORF1b is only expressed by ribosomal −1 frame shifting due to a slippery sequence and pseudoknot structure in the overlapping ORF1a/ORF1b junction (Allende *et al.,* 1999; den Boon *et al.,* 1991; Brierly *et al.,* 1989; Meulenberg *et al.,* 1993; Nelsen *et al.,* 1999; Wootton *et al.,* 2000). The catalytic domains and cleavage sites for EAV ORF1 have been identified. The EAV proteases, located within nsp1, nsp2, and nsp4, have been shown to cleave EAV ORF1ab into 12 nonstructural proteins (nsps), 8 in ORF1a and 4 in ORF1b (den Boon *et al.,* 1995; Snijder *et al.,* 1992, 1993a,b; Snijder and Meulenberg, 1998; van Dinten *et al.,* 1996, 1999; Wassenaar *et al.,* 1997). EAV nsp1 autocatalytically cleaves the ORF1 protein immediately downstream between G260 and G261; nsp2 is proposed to cleave far downstream between two glycine residues located at EAV amino acids 1367 and 1368, and nsp4, the major protease, cleaves ORF1 between amino acids glutamine and glycine (EG) or glutamine and serine (ES) (Ziebuhr *et al.,* 2000). Based on significant homology in the catalytic domains and in predicted cleavage sites, it was surmised that PRRSV polymerase may undergo similar proteolytic processing as that of EAV (Snijder and Meulenberg, 1998; van Dinten *et al.,* 1999; Wassenaar *et al.,* 1997; Ziebuhr *et al.,* 2000). The four predicted ORF1b nonstructural polypeptides comprise a putative RNA-dependent RNA polymerase (POL or nsp9), a protein (nsp10) containing a putative metal-binding domain (MBD) and nucleoside triphos-

0042-6822/02 $35.00

phate binding or helicase motif (HEL), and two proteins of unknown function (nsp 11 and 12). Nsp11 contains a domain (CORONA) that is conserved in all nidoviruses (Allende *et al.,* 1999, 2000; den Boon *et al.,* 1991; Godeny *et al.,* 1993; Gorbalenya *et al.,* 1989; Herold *et al.,* 1996; Meulenberg *et al.,* 1993; Nelsen *et al.,* 1999; Shen *et al.,* 2000; Snijder and Meulenberg, 1998; van Dinten *et al.,* 1996, 1999; Wootton *et al.,* 2000).

Despite extensive research on the molecular and biological properties of PRRSV, there are important aspects of the disease and biology that remain unclear. The role of the nonstructural genes encoded in ORF1ab in viral replication, pathogenesis, and immunity have not been demonstrated. This information is necessary to devise effective strategies to prevent and control PRRSV infection of swine. The knowledge available for the genes encoded in ORF1ab is limited to sequence information for a few virus isolates (Allende *et al.,* 1999, 2000; Jiang *et al.,* 2000; Meulenberg *et al.,* 1993; Nelsen *et al.,* 1999; Shen *et al.,* 2000; Wootton *et al.,* 2000) and predictions on their function based on sequence homology and studies on EAV and coronaviruses (Gorbalenya *et al.,* 1989; Herold *et al.,* 1996; Snijder and Meulenberg, 1998; van Dinten *et al.,* 1999). To elucidate the role of the nonstructural genes of arteriviruses in virus replication, previous studies have been done with EAV (12.7 kb) to develop and characterize infectious clones and their derivative mutants (de Vries *et al.,* 2000; van Dinten *et al.,* 1997, 2000; van Marle, 1999). These studies have provided important insights as to the critical role of the genes encoded in ORF1ab in arterivirus replication. However, PRRSV is genetically divergent from EAV, possessing only approximately 41% (ORF1a) to 48% (ORF1b) nucleotide identities to the sequenced EAV cell-adapted avirulent strain (Nelsen *et al.,* 1999). In addition, infectious clones of PRRSV have been more difficult to prepare and analyze, apparently due to the increased genomic size of PRRSV (15.1–15.4 kb), the restricted cell tropism of this virus, and the difficulty in transforming these permissive cells with nucleic acids (Meulenberg *et al.,* 1998). We have chosen a virulent field isolate of PRRSV to explore phenotypic properties of this virus as it exists in nature. To demonstrate and characterize PRRSV ORF1b polypeptides, we have generated recombinant individual nsp proteins that were then analyzed under controlled conditions. This article describes the first functional studies of the putative PRRSV helicase.

RESULTS

Cloning and expression of PRRSV ORF1b polypeptides

Two overlapping ORF1b gene segments were amplified by RT-PCR and designated CF and IH. These gene segments were cloned and confirmed to be PRRSV-14-specific nucleotides by sequence analysis. The nucleotide sequence of PRRSV-14 ORF1b has been deposited in GenBank (Accession No. AF298771). Nucleotide sequence comparison of PRRSV-14 ORF1b revealed that this isolate is closely related to PRRSV-NA strains (data not shown). Sequence analysis also determined that the predicted cleavage sites for PRRSV ORF1b were maintained in isolate PRRSV-14 (Allende *et al.,* 1999; Nelsen *et al.,* 1999). These predicted cleavage sites appear to be well conserved among PRRSV strains (Table 1).

TABLE 1

Predicted Cleavage Sites for PRRSV ORF1b Protein

Cleavage site	PRRSV isolates	Amino acid sequence
Nsp9/10	North American	LRSNYEGKKSRVC
	European	LRShnEGKKfRhC
Nsp10/11	American	AICADLEGSSSPLP
	European	AcsAsLEGScmPLP
Nsp11/12	American	TAYFQLEGRYFTWY
	European	TAYFQLEG..1TWs

Note. ORF1b amino acid alignment of North American and European isolates (GenBank Accession Nos. are indicated in the text) was performed using the Pileup program of SeqWeb Version 1.2 of the Wisconsin Package Version 10.1. The predicted cleavage sites are underlined and based on sequence homology to the predicted sites described for EAV (Meulenberg *et al.,* 1993; Nelsen *et al.,* 1999; van Dinten *et al.,* 1996, 1999). Lowercase indicates amino acid difference at that position compared to the reference NA strain.

Genome clones CF and IH both contained an overlapping unique *Sac*I site that was used to generate a 5262-nt CH fragment, which comprised all ORF1b flanked by minimal ORF1a sequence at the 5′ end and by a small amount of ORF2 sequence at the 3′ end. The CH fragment was cloned and used as a template to generate PCR-amplified ORF1b nsp gene fragments (Fig. 1A). These gene fragments were cloned into pRSET-B plasmids for protein expression and designated pTPRRSV14 nsp9–12. Western blot analysis with T7.10 Ab demonstrated that the produced recombinant proteins corresponded to polypeptides of the predicted molecular size (Fig. 1B). To confirm the specificity of the individual nsps, antipeptide rabbit sera were generated as described under Materials and Methods. Western blot analyses with nsp10 antipeptide rabbit sera (α-HEL, Fig. 1B) or other gene-specific anti-peptide sera (data not shown) demonstrated the specificity of PRRSV-14-specific individual nsps.

Experiments were conducted to obtain soluble recombinant PRRSV-14 ORF1b proteins. Optimal conditions for nsp10, which is predicted to have RNA helicase and ATPase functions (Meulenberg *et al.,* 1993), were obtained with the *Escherichia coli* strain BL21(DE3)pLysE, which has been designed to have more stringent expres-

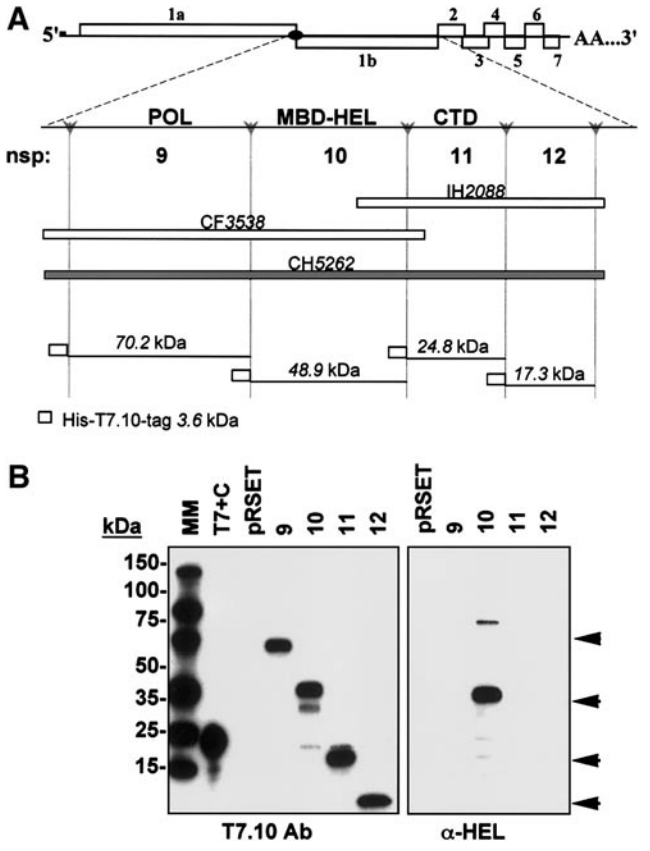

FIG. 1. Cloning and expression of PRRSV-14 ORF1b nonstructural proteins (nsp). (A) Schematic representation of the strategy for cloning and expressing PRRSV ORF1b nsps. Genome organization of PRRSV with the ORF1b region shown expanded below. Motifs identified by sequence comparison are indicated. Nsp9, 10, 11, and 12 gene segments are indicated by arrows. The letters on the open bars indicate the primers used for amplification and the numbers in italics represent the predicted molecular size of the amplified products. The IH- and CF-amplified gene segments were selected for cloning and sequencing. The cloned IH and CF gene fragments were consequently ligated at the *Sac*I restriction site to generate the CH fragment (represented by the cross-hatched bar) that contains the complete ORF1b gene of PRRSV-14. The recombinant polypeptides from PRRSV-14 ORF1b that were expressed in the prokaryotic system are presented by lines. The number in italics on the lines represent the predicted molecular size in kilodaltons (kDa) of PRRSV-14 ORF1b polypeptide fragments. The histidine (His)-T7.10 tag derived from the expression vector increased the molecular size in approximately 3.6 kDa. (B) Western blot analysis of the expressed recombinant proteins with the indicated antibodies described in the text. Molecular markers (MM) are indicated by the numbers at the left in kDa. A positive control protein for the monoclonal antibody T7.10 was included (T7+C). As negative control, bacterial extracts that were transformed with empty plasmids (pRSET) were included to test each antibody. The protein bands that were specifically recognized by the antibodies and had the expected molecular size of the predicted polypeptide are indicated by arrows.

sion of the T7 polymerase. In addition, culturing of transformed bacteria at 22°C and the use of reduced-nutrient media further improved expression. Under these conditions and after 3 h of IPTG induction, approximately 60–80% of expressed recombinant nsp10 protein was soluble.

Efforts were directed to obtain purified nsp10 and to characterize its predicted NTPase function and demonstrate its helicase activity. To obtain purified recombinant PRRSV-14 helicase, proteins in soluble extracts from bacteria transformed with pTPRRSV14-nsp10 were adsorbed by affinity to cobalt or nickel resins and eluted as described. Samples obtained in the last elution fractions from nickel columns provided a highly purified helicase-soluble protein preparation (>95% pure based on Coomassie blue staining, Fig. 2). Protein preparations obtained with cobalt resins also yielded adequate yields but had reduced ATPase activity compared to nickel affinity-purified protein (data not shown). Therefore, nickel affinity-purified nsp10 helicase was used for the characterization of its inherent ATPase and helicase activities. With similar conditions, soluble nsp11 and nsp12 were obtained (data not shown) and used as controls in the subsequent experiments as indicated.

NTPase activity of recombinant PRRSV-14 helicase

As initial proof of helicase-like activity, experiments were performed to test the ability of purified PRRSV-14 nsp10 protein to hydrolyze radiolabeled ribonucleotides in the presence or absence of polyribonucleotides. From the autoradiographic films of the chromatographs (Fig. 3), it was apparent that PRRSV nsp10 helicase hydrolyzed all four nucleotides in the absence of polynucleotides. Polynucleotides did not appear to significantly affect the level of nucleotide hydrolysis, except for a slight reduction in the level of hydrolysis of CTP in the presence of poly(U). To further characterize the NTPase function of PRRSV nsp10 helicase, the subsequent studies were performed with ATP as substrate.

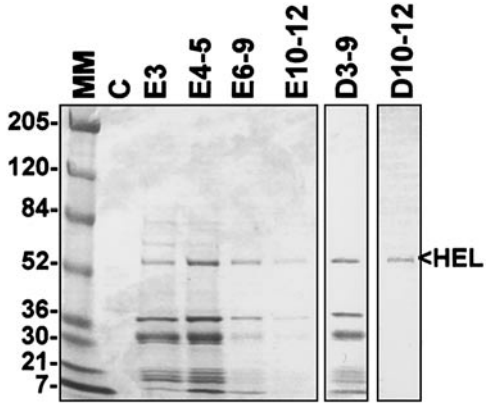

FIG. 2. Metal-affinity purification of PRRSV-14 helicase. Elution fractions (E) containing the recombinant PRRSV-14 ORF1b nsp10 or helicase polypeptide were subjected to SDS–PAGE and Coomassie blue staining. Elution fractions 3 to 9 and 10 to 12 were pooled and dialyzed. The dialyzed protein samples are indicated by D. Molecular markers (MM) are indicated at the left in kDa. The T7.10 control protein (C) was also included.

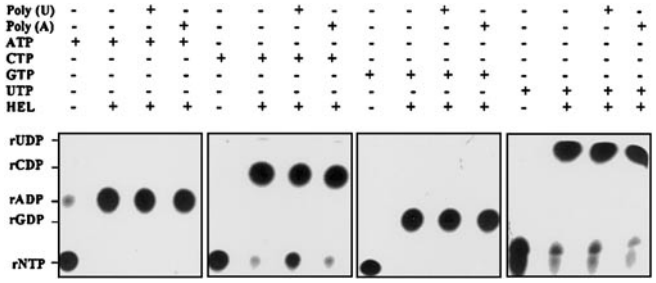

FIG. 3. PRRSV putative helicase has NTPase activity in the absence of polynucleotides. The NTPase assay was performed as described under Materials and Methods with 0.01 μCi/μl of the radiolabeled nucleotides ATP, CTP, GTP, or UTP in the presence (+) or absence (−) of 0.1 μg/μl poly(U) or poly(A) and 0 (−) or 5 ng/μl (+) of protein (HEL). The migration of the triphosphate nucleotide substrates and diphosphate nucleotide products are indicated at the left.

Characterization of recombinant nsp10 helicase ATPase activity

The level of ATPase activity in recombinant PRRSV helicase was compared to the ATPase activity in control samples. The control samples were obtained following the same procedure used for purification of recombinant helicase and consisted of protein preparations (equalized by protein concentration) obtained from bacteria transformed with one of the following plasmids: (1) empty pRSET, (2) pTprrsvnsp11, or (3) pTprrsvnsp12. The results demonstrated that the hydrolysis of ATP appeared specific for recombinant nsp10 (PRRSV helicase) and not for possible contaminating bacterial proteins. These results also established that both predicted nsp11 and predicted nsp12 products lacked a specific ATPase activity (Fig. 4).

The ATPase activity of PRRSV helicase was shown to be dependent on recombinant protein concentration (Fig. 4). PRRSV helicase ATPase activity was also determined to be dependent on pH (optimal pH range was between 7.5 and 8.5) and influenced by the assay buffer used (Fig. 5A). With Tris buffer, the ATPase activity of PRRSV helicase was stable over a broader pH range than with the other buffers tested (Fig. 5A). There was no significant differences seen in the level of ATPase activity using Tris buffer concentrations in the range of 10 to 100 mM (data not shown). Further characterization of the ATPase activity was performed using 25 mM Tris buffer at pH 8.0. PRRSV helicase activity was dependent on the presence of divalent ions, as the presence of EDTA inhibited the recombinant proteins' ATPase activity in a dose-dependent manner (Fig. 5B). In addition, there was no ATPase activity observed in the absence of divalent ions (Fig. 5C). Optimal ATPase activity was detected at 1–2 mM for all the four divalent ions tested. Whereas the level of ATPase activity of PRRSV helicase consistently remained stable over a broader range of $MgCl_2$ concentrations, increasing concentrations of $MnSO_4$ inhibited the activity in a dose-dependent manner and to a greater extent than the other divalent ions tested (Fig. 5C). Lastly, the ATPase activity of PRRSV helicase was very sensitive to temperature. Optimal activity was detected between 25 and 30°C. The ATPase activity was significantly reduced at 37.5°C and was only detected at background levels at temperatures at and above 40°C and completely abolished at 60°C (Fig. 5D). Kinetic analysis of recombinant helicase ATPase activity revealed dependence on time (Fig. 6A) and substrate concentration (Fig. 6B). The Michaelis–Menten constant (K_M) for the ATPase activity of PRRSV helicase was determined to lie in the range of 6–13 mM ATP, with a maximum velocity of 1.3–2 mM ATP hydrolyzed per min (Fig. 6C).

To assess whether the level of ATPase activity would be affected by the presence of polynucleotides, kinetic analysis was performed in the presence or absence of poly(U). Poly(U) significantly enhanced the ATPase activity of PRRSV helicase at a given ATP level (Fig. 7A). Although maximum velocity of enzymatic activity was not reached, comparison of the initial velocities of the relative ATPase activities showed that the presence of poly(U) increased the K_M and V_{max} at least 19- and 24-fold, respectively. However, at low ATP concentrations, poly(U) did not have an effect or tended to reduce the ATPase activity (Table 2). The fold increase in the level of ATP hydrolyzed induced by poly(U) was in a close linear proportion ($r^2 = 0.9817$) to the concentration of ATP substrate (Fig. 7B). These data indicate that the effect of polynucleotides on the ATPase activity of PRRSV is dependent on ATP substrate concentration. This result also explains our initial findings (Fig. 4), in which no apparent effect of the polynucleotides was detected when the ATP concentration was limited and the level of ATPase activity present in the assay was nearly 100% of the substrate.

Last, the effect of the presence of other mononucleotides on the level of ATPase activity was ascertained using the bioluminescence detection method (McElroy and DeLuca, 1983). This assay has been shown to spe-

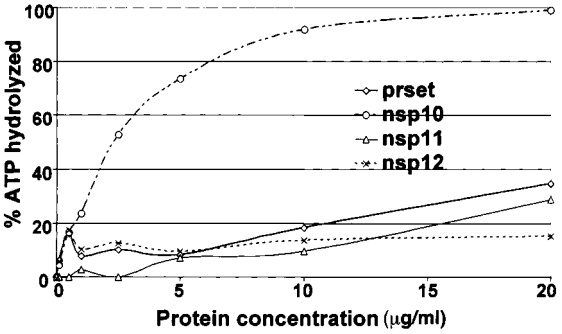

FIG. 4. Specificity of the ATPase activity of PRRSV-14 helicase. The specificity of the ATPase activity was determined by testing the indicated protein concentrations of purified recombinant proteins prepared as described in the text. The ATPase assay was performed using 0.1 μM of ATP substrate and the level of ATP remaining in the samples was measured after 30 min incubation. The level of ATPase activity is expressed as the percentage of ATP hydrolyzed in the ATPase assay. Data represent the mean ± standard deviation of triplicate samples.

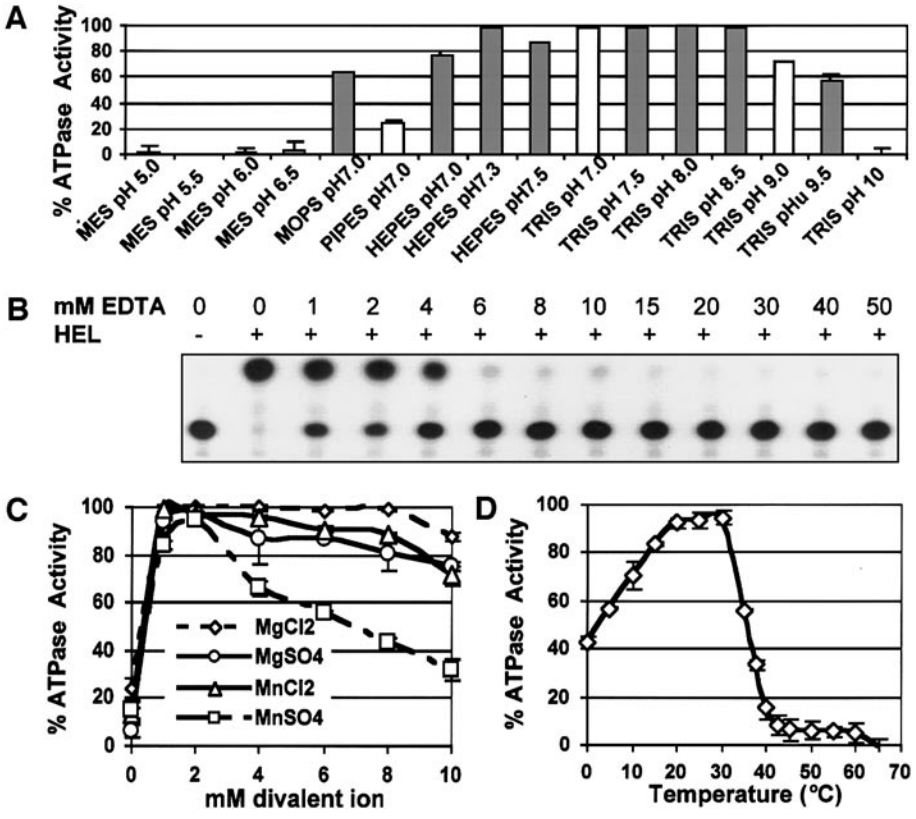

FIG. 5. Characterization of the ATPase activity of PRRSV helicase. (A) Effect of pH on the ATPase activity. (B) Effect of various concentrations (in mM) of EDTA on the ATPase activity of PRRSV helicase (HEL) when tested in the presence of 3 mM $MgCl_2$ as determined by TLC. (C) Requirement and concentration effect of divalent ions on the ATPase activity. (D) Effect of temperature on the ATPase activity. The percentage (%) of the ATPase activity is expressed as the percentage of the total ATP substrate that was hydrolyzed in the assay. Data in A, C, and D represent the mean ± standard error of triplicate samples tested under the same experimental conditions. The concentration of ATP substrate used in these assays was 0.1 μM. At this substrate concentration, 5 ng/μl of the highly purified PRRSV helicase hydrolyzed nearly 100% of the ATP substrate under optimal conditions after 30 min incubation.

cifically detect ATP (Moyer and Henderson, 1983). In addition, we confirmed that the measurement of ATP by the bioluminescence method was not affected by the presence of CTP, GTP, or UTP (data not shown). As shown in Fig. 8, CTP, GTP, and UTP inhibited the level of ATP hydrolysis by PRRSV helicase only when they were present at concentrations at least 10-fold higher than the ATP substrate. This result confirms that PRRSV nsp10 helicase protein can interact with all four nucleotides and, furthermore, this helicase protein may have a higher affinity for ATP than for the other nucleotides.

Unwinding properties of PRRSV helicase

To demonstrate whether recombinant PRRSV helicase possessed functional RNA unwinding activity, various substrates were designed and tested in a standard helicase assay. These substrates consisted of two partially complementary RNA strands containing single-stranded (ss) regions at the 3′ or 5′ ends of one or both strands. One set of substrates designed to contain single-strand regions at both 3′ and 5′ ends did not initially form the expected partial duplex structures under initial hybridization conditions. One explanation is that these long oligonucleotides are predicted to form secondary structures (energies of −25 to −30 kcal/mol; data not shown) and therefore might not have initially annealed to the other strand. However, duplexes or other higher ordered structures appear to form in the presence of recombinant helicase (data not shown). One suggestion for this result is that PRRSV helicase first promoted unwinding of initial interoligonucleotide structures, then winding to form the expected duplexes, and/or introducing secondary structures in the labeled RNA strand.

To further analyze the predicted helicase activity of the PRRSV nsp10 protein, experiments were performed using duplex substrates prepared with synthetic oligonucleotides containing single-strand regions at the 3′ or 5′ ends and short duplex regions (21 and 24 bp). Results obtained with RNA 3′Duplex and 3′3′Duplex indicated that PRRSV helicase lacked 3′-to-5′ unwinding activity (Fig. 9A). In contrast, results with the RNA 5′Duplex revealed that PRRSV helicase has unwinding activity in the 5′-to-3′ orientation (Fig. 9B). The 5′-to-3′ orientation of the unwinding activity of the PRRSV helicase was

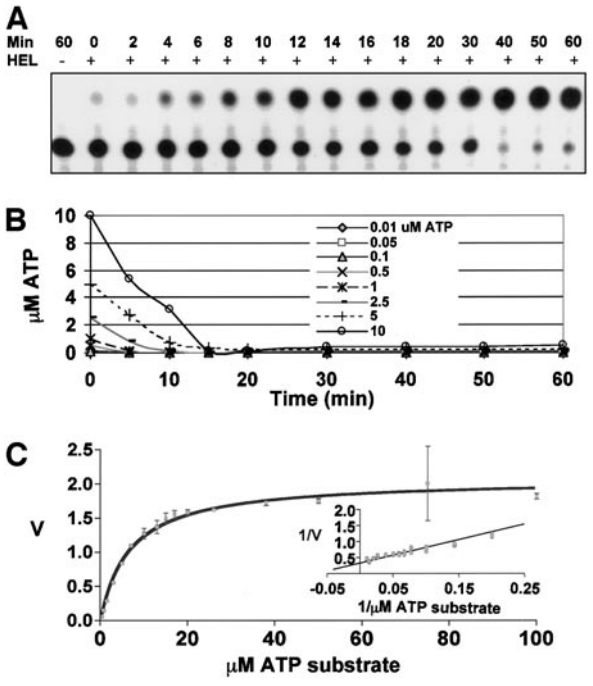

FIG. 6. Kinetics analysis of the ATPase activity of PRRSV helicase. (A) ATPase activity of PRRSV helicase tested with radiolabeled ATP as substrate at various incubation times. (B) Kinetics analysis of the ATPase activity of PRRSV helicase at various ATP substrate concentrations for the indicated incubation times as determined with the bioluminescence ATP assay. (C) Nonlinear regression analysis (R^2 = 0.9962) of the initial velocity of the ATPase activity of PRRSV helicase. The substrate and product concentrations are expressed in μM. The velocity of the ATPase activity is expressed as the μM product (ATP hydrolyzed) per min. Data represent the mean ± standard error of triplicate separate samples. The Lineweaver–Burk plot of ATP hydrolysis is shown in the inserted graph in C.

further confirmed in experiments using substrates prepared with *in vitro* transcribed RNA that contained single-strand regions at the 5′ end of both strands and duplex regions of 67 bp (5′5′Duplex #1) and 85 bp (5′5′Duplex #2), as shown in Fig. 9B. These results, together with the ATPase data described above, demonstrate that the recombinant PRRSV nsp10 helicase is functionally active and shares the properties reported for helicases of other members of the *Nidovirales* (Seybert *et al.,* 2000a,b).

DISCUSSION

The nonstructural polypeptides encoded in *Nidovirales* ORF1b regions have been predicted to have essential roles in virus replication and gene expression (Allende *et al.,* 1999; Gorbalenya *et al.,* 1989; Meulenberg *et al.,* 1993; Nelsen *et al.,* 1999; van Dinten *et al.,* 1996). Evidence for the significant role of these proteins in arteriviruses has been derived using an infectious clone of EAV (van Dinten *et al.,* 1997, 1999, 2000; van Marle *et al.,* 1999). However, as stated previously, EAV is genetically distinct from other arteriviruses, possessing only approximately 48% nucleotide identity and 53.8% amino acid identity in the ORF1b region when compared to PRRSV-NA (Nelsen *et al.,* 1999). Thus, it is crucial to gather basic information on distantly related arteriviruses to examine variability in ORF1b nucleotide composition and function and to assess outcomes of potential ORF1b region mutations. This study was completed to provide molecular tools to facilitate understanding of the biochemical and functional properties of PRRSV-NA-predicted ORF1b-processed polypeptides.

Accordingly, we have cloned and expressed predicted ORF1b protein products of PRRSV-14 in a prokaryotic system and determined optimal conditions for functional expression of soluble nsp10, nsp11, and nsp12. Of these three polypeptides, nsp10 was chosen for further biochemical characterization, as this predicted protein has been shown by sequence comparison to contain conserved NTPase and helicase domains (Allende *et al.,* 1999; Nelsen *et al.,* 1999; Meulenberg *et al.,* 1993) of the superfamily (SF) 1 of helicases (Kadare and Haenni, 1997; Seybert *et al.,* 2000a,b).

PRRSV-NA nsp10 bears only approximately 45% amino acid similarity to nsp10 of EAV (Nelsen *et al.,* 1999), illustrating remarkable interfamily divergence and rendering possible differences in precise dynamics for this critical protein. The described studies demonstrated that the predicted nsp10 product containing the metal binding and NTPase-helicase domains of PRRSV ORF1b has NTPase activity. The initial NTPase analysis, determined by thin-layer chromatography, revealed that PRRSV helicase hydrolyzes the four ribonucleotides in the absence of polynucleotides. The interaction of the recombinant

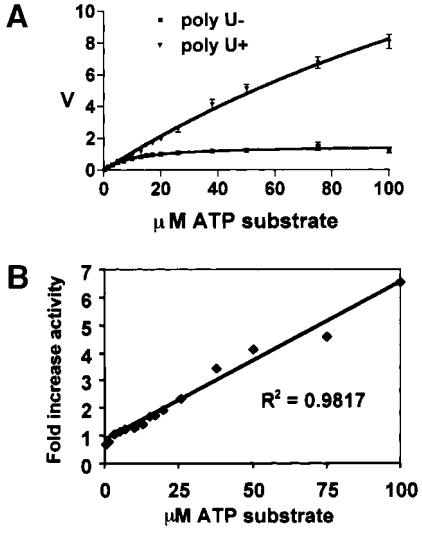

FIG. 7. Effect of poly(U) on the kinetics of the ATPase activity of PRRSV helicase. (A) Nonlinear regression analysis of the initial velocity of the ATPase activity of PRRSV helicase in the presence (+) or absence (−) of poly(U). The velocity (V) is expressed as the μM concentration of ATP hydrolyzed per min. (B) Linear regression analysis of the poly(U)-induced fold increase in the ATPase activity (total μM ATP hydrolyzed in the assay) of PRRSV helicase as a function of the concentration of ATP substrate.

TABLE 2

The Effect of Poly(U) on the ATPase Activity of PRRSV Helicase Is Dependent on the Concentration of ATP Substrate

Substrate (μM ATP)	Mean μM ATP hydrolyzed		Fold effect	P*
	Poly(U)−	Poly(U)+		
0.30	0.27 (0.01)	0.18 (0.01)	0.67	0.01
0.75	0.59 (0.02)	0.42 (0.04)	0.71	0.08
1.50	1.10 (0.02)	0.87 (0.02)	0.79	0.03
3.00	1.70 (0.02)	1.79 (0.02)	1.05	0.03
5.00	2.47 (0.18)	2.84 (0.11)	1.15	0.14
7.00	2.84 (0.21)	3.55 (0.19)	1.25	0.17
10.00	3.66 (0.17)	4.73 (0.05)	1.29	0.04
13.00	4.13 (0.34)	5.92 (0.21)	1.43	0.08
15.00	4.71 (0.15)	7.87 (0.06)	1.67	<0.01
17.00	4.85 (0.34)	8.50 (0.42)	1.75	0.02
20.00	5.06 (0.24)	9.66 (0.39)	1.91	0.02
26.00	5.45 (0.48)	12.80 (0.85)	2.35	0.03
38.00	6.03 (0.43)	20.59 (1.68)	3.41	0.01
50.00	6.23 (0.42)	25.55 (1.39)	4.10	0.01
75.00	7.40 (1.25)	33.75 (1.76)	4.56	0.01
100.00	6.18 (0.90)	40.29 (2.24)	6.52	<0.01

Note. The ATPase assay was performed as described under Materials and Methods at the indicated ATP concentrations in the presence (+) or absence (−) of poly(U) in triplicate.

* Statistical significance was determined by paired two-sample *t*-test with alpha at 0.05.

PRRSV helicase with the nucleotides was confirmed by demonstrating that the presence of excess GTP, CTP, and UTP inhibited the level of ATP hydrolysis. The ability of PRRSV helicase to catalyze hydrolysis of different nucleotides is a characteristic shared by various reported viral helicases (Bisaillon *et al.,* 1997; Kadare *et al.,* 1996; Li *et al.,* 1999; Preugschat *et al.,* 1996; Rikkonen *et al.,* 1994). We demonstrated that the activity observed for the recombinant his-tagged nsp 10 is specific for the helicase because the recombinant PRRSV ORF1b nsp11 and nsp12 polypeptides that were expressed and purified under the same conditions as PRRSV helicase did not have specific ATPase activity. Although ATPase activity has been previously reported for the human coronavirus 229E helicase (Heussip *et al.,* 1997; Seybert *et al.,* 2000a), a member of the order *Nidovirales,* and more recently for EAV (Seybert *et al.,* 2000b), this is the first study reporting the characterization of the NTPase activity of the putative helicase of PRRSV.

The characterization of the ATPase activity revealed some features of PRRSV helicase that are common among known viral helicases such as the requirement for divalent cations and sensitivity to extreme pH and temperatures. In contrast to other viral helicases (Bisaillon *et al.,* 1997), PRRSV helicase appears to be extremely sensitive to temperatures above physiological levels. This finding suggests that viral or cellular factors may be required to stabilize PRRSV helicase function. The ATPase activity of PRRSV helicase was also dependent

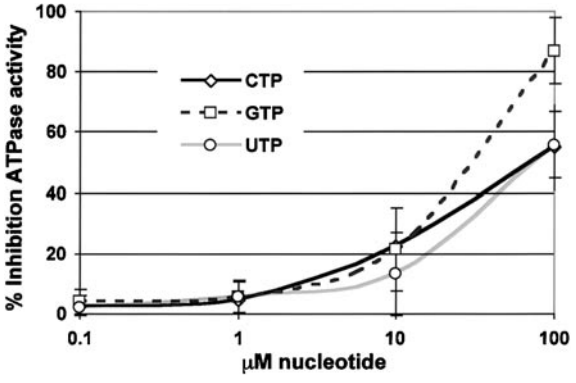

FIG. 8. Effect of CTP, GTP, and UTP on the ATPase activity of PRRSV helicase. The ATPase assay was performed with 0.1 μM ATP substrate in the presence of the indicated concentrations (in μM) of CTP, GTP, or UTP as described in the text. The level of ATP hydrolysis was determined after 30 min incubation by the bioluminescence ATP detection method. Data are expressed as the mean of the percentage inhibition of ATPase activity determined from three separate samples. Error bars indicate the standard deviation of the mean.

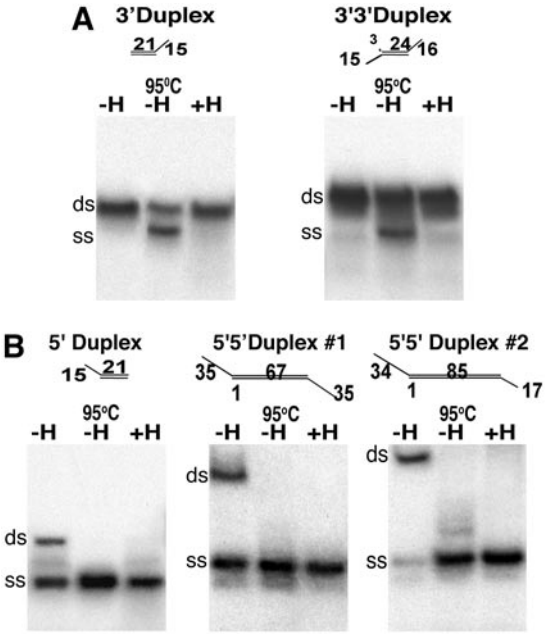

FIG. 9. PRRSV helicase activities. RNA substrates were generated by annealing two partially complementary RNA strands for use in a standard helicase (hel) assay. RNA substrate predicted duplex structures are indicated by diagrams above each assay result. A sample lacking PRRSV helicase (−H) was included to indicate migration of intact radiolabeled duplex, and denatured substrates (−H, 95°C) were included to indicate migration of unduplexed labeled short strand. Migration of substrates after the helicase assay is indicated on each electropherogram as single-stranded (ss) or double-stranded (ds) oligomers. (A) Results of the helicase assay with substrates containing 3′ single regions at one (3′Duplex) or both (3′3′Duplex) strands and duplex regions of 21 and 24 bp, respectively. (B) PRRSV helicase activity displaced the labeled short strand of 5′ tailed RNA substrates with duplex lengths of 21 (5′Duplex), 67 (5′,5′Duplex-#1), and 85 bp (5′5′Duplex-#2).

on protein concentration. Although the presence of polynucleotides was not required for detecting the NTPase activity of PRRSV helicase using the standard TLC method, poly(U) had a significant effect on this activity when the activity was measured at various ATP substrate concentrations. Interestingly, the effect of poly(U) in the ATPase activity of PRRSV helicase was dependent on the substrate concentration. At ATP concentrations lower than the estimated K_M, poly(U) had an inhibitory effect, whereas at higher ATP concentrations, poly(U) had a stimulatory effect on the ATPase activity of PRRSV helicase. It was also interesting to note that the level of effect of poly(U) was in a close linear relationship with the ATP substrate concentration.

The substrate concentration-dependent modulatory effect of polynucleotides on the ATPase activity of PRRSV helicase found in this study has not been previously described. Data reported for other viral helicases are consistent with a stimulatory effect that varies depending on the type of helicase and polynucleotide used (Rikkonen *et al.,* 1994; Tamura *et al.,* 1993). The level of nucleic acid stimulation reported for the known members of the viral SF1 and SF3 helicases has only been in the range of a twofold increase, whereas higher levels of stimulation have been reported for SF2 helicases (Kadare and Haenni, 1997). The ATPase activity of the human coronavirus 229E, which belongs to the same *Nidovirales* order as PRRSV, was found to be highly stimulated with polynucleotides and the major stimulatory effect was found with poly(U), which increased the NTPase activity of the helicase up to 50-fold (Heusipp *et al.,* 1997; Seybert *et al.,* 2000a). A 20-fold increase in the ATPase activity by polynucleotides was found for the EAV helicase (Seybert *et al.,* 2000b). For PRRSV helicase we found that whereas the overall effect of poly(U) on the K_M and V_{max} reached levels of 19- and 24-fold increase, respectively, the effect on the amount of ATP hydrolyzed varied from ~0.6-fold (at 0.3 μM ATP substrate) to 6.5-fold (at 100 μM ATP substrate). Experimental data analyzing the effect of polynucleotides under the range of ATP substrate concentrations used in this study have not been reported for other viral helicases. Therefore, it is not clear whether our findings represent a unique feature of PRRSV helicase. We suggest that the modulatory effect of poly(U) on the ATPase activity of PRRSV helicase discovered in this study may have biological relevance regarding virus replication and gene expression. It is tempting to speculate that if PRRSV helicase is involved in the processes of its genome replication and transcription, as suggested by the studies with the mutant EAV infectious clones (van Dinten *et al.,* 1997, 2000; van Marle *et al.,* 1999), PRRSV helicase needs to be regulated to achieve a balance between nucleotide hydrolysis and viral RNA synthesis. Analysis of the crystal structure of PRRSV helicase will be important to determine whether the regulatory effect of polynucleotides in the ATPase activity of PRRSV helicase is dependent on conformational changes differentially induced by various ratios of ATP substrate to polynucleotide bound to the protein.

To further characterize PRRSV helicase function in terms of its major predicted role in RNA winding, studies analyzing the ability of the protein to interact with various substrates were performed. The recombinant helicase did not exhibit 3′ to 5′ unwinding activity on synthesized oligomer duplexes of 22 or 24 bp and single-strand regions of 15–16 nucleotides. The PRRSV helicase did demonstrate 5′-to-3′ unwinding activity on duplexed substrates with single-stranded segments on one or both 5′ ends. These results are consistent with the 5′-to-3′ unwinding properties found for EAV (Seybert *et al.,* 2000b) and HCoV (Seybert *et al.,* 2000a), supporting the finding that *Nidovirales* SF1 helicases are closely related with functional properties different to those of other viral helicase families.

This study provides the first evidence on both ATPase and helicase-like activities of PRRSV helicase and suggests a regulatory role of polynucleotides on its ATPase activity and unwinding properties. The molecular tools developed in this study will be useful for further studies directed to understand the role of the predicted intermediate ORF1b gene protein products in PRRSV replication.

MATERIALS AND METHODS

Virus selection, purification, and RNA isolation

A PRRSV isolate, designated PRRSV-14, was obtained from the National Veterinary Services Laboratories (NVSL, Ames, IA). Selection of isolate PRRSV-14 was based on its clinical history and its ability to replicate well in the MARC-145 cell line (Kim *et al.,* 1993). The virus was isolated from the serum of an 8-day-old piglet exhibiting interstitial pneumonia. The piglet had come from an Alabama farm experiencing a reproductive disease outbreak in March of 1996. PRRSV-14 was propagated in MARC-145 cells to passage level 9–10. Culture fluid containing virions was concentrated by ultracentrifugation through a 0.5-M sucrose cushion and further purified by sucrose gradient centrifugation as described (Bautista *et al.,* 1996). Viral RNA was extracted from the purified virus with Trizol reagent (GIBCO-BRL), concentrated by alcohol precipitation, suspended in RNase-free double distilled water, and stored at −70°C until analyzed.

RT-PCR, cloning, and sequencing analysis of PRRSV-14 ORF1b genomic segments

PRRSV-14 gene fragments containing ORF1b sequences were amplified by RT-PCR. Reverse transcription was performed in a 100-μl reaction containing 1 μg of purified viral RNA, 0.25 μg random hexamers, and 1000 U Superscript II reverse transcriptase (GIBCO-BRL), following the manufacturer's recommendations. Polymer-

TABLE 3

Primers Used for Cloning PRRSV-14 ORF1b Genes

Name	Sequence
Primers for RT-PCR cloning[a]	
C-VR7499F[c]	5′-CTTGGTCCCCGTCAACCCAGAG
F-VR11036R	5′-TTGACACCACGGGCCAGTGA
H-VR12760R	5′-ATTGGAACCCGCAACCACAGCA
I-NE10695F	5′-GCCATCACCAGGGCAAGACACG
Primers for cloning PRRSV ORF1b into PRSET-B[b]	
PRRSVpolF	5′-GAGCTCG AGACTAGCCGCCAGCGGCTTGACCCGC
PRRSVpolR	5′-CATGGTACCTCATCACTCATAATTGGACCTGAGTTTTTC
PRRSVhelF	5′-AAGGATCCGGGGAAGAAGTCGAGAGTGTGCGGG
PRRSVhelR	5′-CATGGTACCTCATCATTCTAGATCAGCACAAATGGCGCG
PRRSVctdF	5′-AAGGATCCGGGGTCGAGCTCTCCGCTCCCCAAG
PRRSVctdR	5′-CATGGTACCTCATCATTCAAGTTGGAAATAGGCTGTTTT
PRRSVnsp12F	5′-AAGGATCCGGGTCGCTATTTCACCTGGTATCAG
PRRSVnsp12R	5′-CATGGTACCTCATCAATTCAGGCCTAAAGTTGGTTC

[a] Primers were designed based on published nucleotide sequences from PRRSV isolates VR = ATCC-VR-2332 (26) and NE = 16244B (1).
[b] Primers were designed based on PRRSV-14-specific sequences.
[c] F = forward primer; R = reverse primer.

ase chain reactions (PCR) were performed in 50 μl reactions using 2 μl viral cDNA, 200 μM dNTPs, 1 U high-fidelity Vent (New England Biolabs), and various set of primers (Table 3) according to the strategy depicted in Fig. 1A. The reactions were performed by an initial denaturation for 5 min at 94°C, followed by 30 cycles and 10 min final extension at 72°C. The cycles consisted of denaturation at 95°C for 45 s, annealing at 58°C for 1 min, and extension at 73°C for 2.10 min + 10 s/cycle. The extension time for gene products longer than 3000 nt was performed for 3.2 min + 10 s/cycle. Two overlapping fragments, designated CF and IH (Fig. 1A), were cloned into the pCRBlunt Vector system (Invitrogen). Plasmid DNA from selected CF and IH clones were purified using a plasmid purification kit (Qiagen) according to the manufacturer's instructions and confirmed by enzymatic restriction and sequence analysis. Sequence analysis was performed with plasmid-specific primers at the automated sequence facility at Eli Lilly and Co., Indianapolis, IN. PRRSV sequences used for nucleotide and amino acid comparison included published GenBank sequences U87392 (VR-2332; Nelsen *et al.,* 1999), AF066183 (RespPRRS; Yuan *et al.,* 2001), AF066384 (PrimePac; Yuan *et al.,* 1999), AF184212 (SP, Shen *et al.,* 2000), AF176348 (PA8, Wootton *et al.,* 2000), and M96262.1 (Lelystad; Meulenberg *et al.,* 1993).

Cloned CF and IH fragments were joined at a unique *Sac*I restriction site to generate a 5262-nt CH fragment (Fig. 1A), which comprised the last 182 nt of ORF1a, all of ORF1b, and the first 711 nt of ORF2. Four CH clones (CH2, CH11, CH18, and CH37) were confirmed for proper frame and orientation by restriction digest and sequence analysis. The CH2 clone was used as a template for further ORF1b nsp gene subcloning. Gene fragments encoding predicted ORF1b nsps (nsp 9 to 12) were amplified by PCR and cloned into the pCRBlunt vector using PRRSV-14-specific primers (Table 3) designed to contain restriction sites for cloning into the prokaryotic pRSET-B expression vector (Invitrogen). pRSET-B bacterial expression vector cloning was performed following standard techniques (Sambrook, 1989). Briefly, the gene fragments were inserted into the *Bam*HI and *Kpn*I sites of the pRSET. The recombinant pRSET plasmids containing ORF1b nsp genes were confirmed for proper orientation and frame by enzymatic restriction analysis and by sequencing the region at the insertion sites. The recombinant plasmids were designated pT-prrsvnspN, where N corresponded to the number of the cloned ORF1b nsp.

Expression analysis of predicted ORF1b nsp, optimization of protein expression, and protein purification

The pRSET vector system allows the expression of recombinant proteins via transcription by IPTG-induced T7 polymerase. ORF1b nsps were expressed as recombinant proteins attached at their amino-terminus to a tag containing a polyhistidine peptide, the antigenic peptide T7.10, and an enterokinase cleavage site. Ten to fifty nanograms of recombinant pRSET-B plasmid DNA containing the corresponding ORF1b fragments were placed in *E. coli* BL21(DE3)pLysS- or BL21(DE3)pLysE-competent cells by bacterial transformation following the manufacturer's recommendations (Invitrogen). Expression of soluble recombinant proteins was optimized by culturing transformed bacterial clones at various temperatures, in

different culture media, and by varying IPTG-induction times. Recombinant protein expression was confirmed by Western blot analysis of crude protein extracts with a chemiluminescence detection kit (Boehringer Mannheim) using selected antibodies, including a monoclonal antibody to the polyhistidine peptide (Clontech), a T7.10 tag antibody (Novagen), and peptide-specific polyclonal antisera generated to PRRSV-14 nsp 9, 10, and 11 (described below). After optimal conditions were determined, soluble recombinant proteins were purified from bacterial extracts by affinity to cobalt (Novagen) or Ni-NTA (Qiagen) resins according the manufacturer's recommendations. Recombinant proteins were eluted with 300 mM imidazole. Eluted fractions were subjected to electrophoresis, followed by Coomassie blue staining, and Western blot analysis. Fractions containing the purified recombinant protein of interest were pooled and dialyzed against 50 mM Tris pH 7.5 containing 1% glycerol and 1 mM DTT. Purified proteins were stored at −20°C until further analysis. Purified recombinant protein concentrations were determined by colorimetric assay (Smith *et al.,* 1985) using the BCA Protein Assay Reagent Kit (Pierce) with bovine serum albumin (BSA) as standard.

Antipeptide sera

Antigenic regions for development of antipeptide sera were selected by computer analysis of peptide hydrophobicity/antigenicity indices of the predicted amino acid sequences of PRRSV-14 nsp 9, 10, and 11 genes. The amino acid sequences of the peptides used to generate the antibodies were (C)HRPSTYPAKNSMAGINGRFPTKD for nsp9, (C)EQGLTPLDPGRYQTRRG for nsp10, and (C)REYLDDRERE for nsp11. Peptide synthesis, KHL conjugation, polyclonal rabbit antibody production, and affinity purification of antibodies were contracted with Zymed Laboratories, Inc. Affinity-purified antibodies were preadsorbed with lysates of porcine alveolar macrophages, MARC-145, and *E. coli* cells at 4°C overnight, clarified by centrifugation, filtered through a 0.22-nm filter, and aliquots stored at −20°C. Optimal antibody concentration was determined by testing serial dilutions of antibodies by Western blot of crude protein extracts.

Analysis and characterization of NTPase activity of PRRSV-14 nsp10 (helicase)

The functionality of the recombinant nsp10 helicase was initially determined by assessing NTPase activity on standard thin layer-chromatography (Gwack *et al.,* 1999). Purified protein samples were incubated with 0.1 μCi of α-^{32}P-labeled ribonucleotide in 10 μl of a solution containing 2 mM DTT, 1 mM NaCl, and 100 μg/ml BSA at different conditions. The samples were analyzed under various divalent ion concentrations, temperatures, time periods, protein concentrations, pH conditions, and buffer systems. The divalent ions tested included $MgCl_2$, $MgSO_4$, $MnCl_2$, and $MnSO_4$. Different pH conditions were tested using buffers containing 25 mM MES, 25 mM PIPES, 25 mM HEPES, or 25 mM Tris. Reaction products (2 μl) were spotted onto polyethylenimine (PEI)-cellulose F plates (EM Science). Chromatographs were developed in 0.4 M KH_2PO_4 (pH 3.5), dried, autoradiographed, and analyzed by densitometry or phosphoimaging.

The ATP bioluminescence assay kit CLS II (Boehringer Mannheim) was used for quantitative analysis of nsp 10 ATPase activity. In this assay, the bioluminescent signal emitted by the oxidation of luciferin is directly proportional to the ATP concentration present in the test sample (McElroy and DeLuca, 1983). This assay was performed in triplicate at conditions described above (10-μl reactions) with 0.1 to 1 μM ATP (Promega) as substrate. For kinetic analysis, the level of ATP hydrolysis produced by the recombinant nsp 10 helicase was measured at different concentrations of ATP and at various incubation times. After incubation, the helicase was inactivated at 90°C for 5 min and samples were diluted with 19 vol of 50 mM Tris–HCl pH 8.0 buffer containing 2 mM EDTA. Diluted samples (50 μl) were transferred in triplicate to Microfluor B 96-well flat-bottom plates (Dynex Technologies Inc.). The bioluminescence signal of samples and standards was measured with an Anthos Lucy Microplate Luminometer and Photometer (Labtech International, Ringmer, U.K.). The ATP concentration in the test samples was determined based on a standard curve obtained by the ATP bioluminescence kit manufacturer's instructions (Boehringer Mannheim). The ATPase activity of PRRSV nsp10 in each experimental condition was expressed as the percentage of ATP hydrolyzed calculated by

$$\frac{([\text{ATP control}] - [\text{ATP test}])}{[\text{ATP control}]} \times 100$$

where [ATP test] = concentration of the test samples ATP in the presence of the recombinant; and [ATP control] = concentration of ATP in parallel samples in the absence of the recombinant proteins. Kinetics of the ATPase activity was determined by measuring the concentration of ATP hydrolyzed per min of reaction time. This assay was performed using 100 nM protein in 10 μl reaction buffer containing 25 mM Tris pH 8.0, 3 mM $MgCl_2$, 100 μg/ml BSA, 1 mM NaCl, 2 mM DTT with various concentrations of ATP at 35°C for 5 min. The 5-min incubation was selected because it was within the range at which the rate of ATP hydrolysis was linear (Fig. 7B). The K_M of PRRSV-14 helicase ATPase activity was determined by nonlinear regression analysis of the Michaelis–Menten equation using the Prism program version 3.0 (GraphPad Software) according to the method described by Motulsky (1999).

Preparation of helicase substrates and helicase assay

Duplexed RNA substrates were prepared using both synthetic RNA oligos and *in vitro* transcribed RNA. The synthetic oligonucleotides 5′-GGGAGTAGCTCCAATTCGCCC-3′ (SS1), 5′-TTTTTTTTTTTTTTGGGCGAATTGGAGCTACTCCC-3′ (LS5′), 5′-GGGCGAATTGGAGCTACTCCCTTTTTTTTTT-TTTTT-3′ (LS3′), 5′-CGAGCCATTCTAGGTCAAACCAATT-GCCGCCGTCGACTT-3′ (SS2-3′), and 5′-ACTAGTGGTT-TCACCTAGAATGGCTGCGTCCCTTCTTTTCCTC-3′ (LS2-3′) were purchased from Annovis (Aston, PA). The SS1 and SS2-3′ were labeled at the 5′ end with [γ-^{32}P]-ATP (Amersham, 3000 Ci/mmol) using T4 polynucleotide kinase and purified using the QIAquick Nucleotide removal kit (QIAGEN). Duplexes were generated by annealing the labeled short strands with 10-fold excess unlabeled long strands as described (Seybert *et al.,* 2000b). The following substrates were obtained by annealing RNA oligos for 10 min at 95°C: 5′ Duplex (SS1 + LS-5′), 3′Duplex (SS1 + LS-3′), 3′3′Duplex (SS2-3′ + LS2-3′).

In vitro transcribed RNA was generated using plasmids pGEM-L and pGEM-S as templates. DNA fragments were generated by RT-PCR amplification of strain VR-2332 3′-untranslated region from a previously prepared clone (pTVRsgORF7; unpublished data) using adapter primers (5′-30-*Apa*I: 5′-ACTAG-GGCCCTTAACAAAAAAAAAAAAAAAAAA; 3′-UTR-*Nde*I: 5′-ACTAGCATATGGCACTAGTGATTCCGGAAT; 5′-65-*Apa*I: 5′-ACTAGGGCCCTTAATTGGCGAGAAC-CATGCGGC) to generate 5′-TTAATTGGCGAGAACCAT-GCGGCCGAAATTAACAAAAAAAAAAAAAAAAAAGCG-GCCGCGAATTCCGGAATCACTAGTGCCA-3′ (L fragment) and 5′-TTAACAAAAAAAAAAAAAAAAAAGCGGCCGCGAATT-CCGGAATCACTAGTGCCA-3′ (S fragment). After *Apa*I and *Nde*I digestion, these fragments were cloned into the respective sites of pGEM-T to produce two plasmids (pGEM-S and pGEM-L). These plasmids were subsequently digested with either *Apa*I (SP6 orientation), *Sac*I (T7 orientation), or *Nsi*I (T7 orientation), purified using the QIAquick PCR purification kit (QIAGEN), and blunt-ended prior to *in vitro* transcription. *In vitro* transcription was performed with SP6 and T7 polymerases using RiboMAX Large Scale RNA Production System (Promega). pGEM-S was transcribed in the presence of [α-^{32}P]-UTP (Amersham, 3000 Ci/mmol). Transcripts were treated with DNAse I and purified by two rounds of phenol-chloroform-isoamyl alcohol extraction, followed by two rounds of chloroform-isoamyl alcohol extraction. The substrates 5′3′Duplex#1 (L-SP6-ApaI + S-T7-SacI), 5′5′Duplex#1 (L-T7-SacI + S-SP6-Apa1), 5′5′Duplex#2 (L-T7-NsiI + S-SP6-ApaI), and 5′3′Duplex#2 (L-SP6-ApaI + S-T7-NsiI) were generated by annealing the short radiolabeled transcript with 10-fold excess unlabeled long strand as described (Seybert *et al.,* 2000b).

The unwinding assay was performed in 20 μl reactions containing 400 μM protein, 12 μM substrate in 25 mM Tris buffer (pH 8.0), or HEPES buffer (ph 7.4) containing 5 mM $MgCl_2$, 2 mM DTT, 100 μg/ml BSA, 10% glycerol, 5 mM ATP, and 25 mM NaCl. Reactions were incubated at 30°C for 1 h and stopped by adding 5 μl of 5× loading buffer (5% SDS/15% Ficoll/100 mM EDTA/0.25% bromphenol blue). Controls included in each assay were native (annealed) and denatured (heated at 95°C) substrate in the absence of helicase. The reaction products were analyzed by native TBE–polyacrylamide gel (4–20% gradient gel, Bio-Rad) electrophoresis and autoradiography.

ACKNOWLEDGMENTS

We thank Drs. Stephen Wessman and Randall Levings from the National Veterinary Services Laboratories (NVSL, Ames IA) for providing PRRSV isolates and the MARC-145 cell line. We appreciate Dr. Thomas W. Molitor from the University of Minnesota (St. Paul, MN) for kindly providing PRRSV isolates and anti-PRRSV sera useful in the characterization of PRRSV isolates. The technical advice of Drs. Elcira Villareal and Jesus Gutierrez is deeply appreciated. We thank the personnel from the sequencing facility at Eli Lilly and Co. for help in the automated nucleotide sequencing. The technical assistance of Anita Jackson and the preparation of material transfer agreements by the Lilly's Legal Department are greatly appreciated. Financial support for these studies was provided by Elanco Animal Health, a subsidiary of Eli Lilly and Co., Greenfield, IN.

REFERENCES

Allende, R., Lewis, T. L., Lu, Z., Rock, D. L., Kutish, G. F., Ali, A., Doster, A. R., and Osorio, F. A. (1999). North American and European porcine reproductive and respiratory syndrome viruses differ in non-structural protein coding regions. *J. Gen. Virol.* **80,** 307–315.

Allende, R., Kutish, G. F., Laegreid, W., Lu, Z., Lewis, T. L., Rock, D. L., Friesen, J., Galeota, J. A., Doster, A. R., and Osorio, F. A. (2000). Mutations in the genome of porcine reproductive and respiratory syndrome virus responsible for the attenuation phenotype. *Arch. Virol.* **145,** 1149–1161.

Baker, S. C., Yokomori, K., Dong, S., Carlisle, R., Gorbalenya, A. E., Koonin, E. V., and Lai, M. M. (1993). Identification of the catalytic sites of a papain-like cysteine proteinase of murine coronavirus. *J. Virol.* **67,** 6056–6063.

Bautista, E. M., Meulenberg, J. J., Choi, C. S., and Molitor, T. W. (1996). Structural polypeptides of the American (VR-2332) strain of porcine reproductive and respiratory syndrome virus. *Arch. Virol.* **141,** 1357–1365.

Benfield, D. A., Nelson, E., Collins, J. E., Harris, L., Goyal, S. M., Robison, D., Christianson, W. T., Morrison, R. B., Gorcyca, D., and Chladek, D. (1992). Characterization of swine infertility and respiratory syndrome (SIRS) virus (isolate ATCC VR-2332). *J. Vet. Diagn. Invest.* **4,** 127–133.

Bisaillon, M., Bergeron, J., and Lemay, G. (1997). Characterization of the nucleoside triphosphate phosphohydrolase and helicase activities of the reovirus lambdal protein. *J. Biol. Chem.* **272,** 18298–18303.

Brierley, I., Digard, P., and Inglis, S. C. (1989). Characterization of an efficient coronavirus ribosomal frameshifting signal: Requirement for an RNA pseudoknot. *Cell* **57,** 537–547.

Cavanagh, D. (1997). Nidovirales: A new order comprising *Coronaviridae* and *Arteriviridae. Arch. Virol.* **142,** 629–633.

Collins, J. E., Benfield, D. A., Christianson, W. T., Harris, L., Hennings, J. C., Shaw, D. P., Goyal, S. M., McCullough, S., Morrison, R. B., Joo, H. S., Gorcyka, D., and Chladek, D. (1992). Isolation of swine infertility and respiratory syndrome virus (isolate ATCC VR-2332) in North America and experimental reproduction of the disease in gnotobiotic pigs. *J. Vet. Diagn. Invest.* **4,** 117–126.

Conzelmann, K. K., Visser, N., Van Woensel, P., and Thiel, H. J. (1993). Molecular characterization of porcine reproductive and respiratory syndrome virus, a member of the arterivirus group. *Virology* **193,** 329–339.

de Vries, A. A., Glaser, A. L., Raamsman, M. J., de Haan, C. A., Sarnataro, S., Godeke, G. J., and Rottier, P. J. (2000). Genetic manipulation of equine arteritis virus using full-length cDNA clones: separation of overlapping genes and expression of a foreign epitope. *Virology* **270,** 84–97.

de Boon, J. A., Snijder, E. J., Chirnside, E. D., de Vries, A. A., Horzinek, M. C., and Spaan, W. J. (1991). Equine arteritis virus is not a togavirus but belongs to the coronaviruslike superfamily. *J. Virol.* **65,** 2910–2920.

den Boon, J. A., Faaberg, K. S., Meulenberg, J. J., Wassenaar, A. L., Plagemann, P. G., Gorbalenya, A. E., and Snijder, E. J. (1995). Processing and evolution of the N-terminal region of the arterivirus replicase ORF1a protein: Identification of two papainlike cysteine proteases. *J. Virol.* **69,** 4500–4505.

den Boon, J. A., Kleijnen, M. F., Spaan, W. J., and Snijder, E. J. (1996). Equine arteritis virus subgenomic mRNA synthesis: Analysis of leader-body junctions and replicative-form RNAs. *J. Virol.* **70,** 4291–4298.

Godeny, E. K., Chen, L., Kumar, S. N., Methven, S. L., Koonin, E. V., and Brinton, M. A. (1993). Complete genomic sequence and phylogenetic analysis of the lactate dehydrogenase-elevating virus (LDV). *Virology* **194,** 585–596.

Gorbalenya, A. E., Koonin, E. V., Donchenko, A. P., and Blinov, V. M. (1989). Coronavirus genome: Prediction of putative functional domains in the non-structural polyprotein by comparative amino acid sequence analysis. *Nucleic Acids Res.* **17,** 4847–4861.

Gwack, Y., Yoo, H., Song, I., Choe, J., and Han, J. H. (1999). RNA-stimulated ATPase and RNA helicase activities and RNA binding domain of hepatitis G virus nonstructural protein 3. *J. Virol.* **73,** 2909–2915.

Herold, J., Siddell, S., and Ziebuhr, J. (1996). Characterization of coronavirus RNA polymerase gene products. *Methods Enzymol.* **275,** 68–89.

Heusipp, G., Harms, U., Siddell, S. G., and Ziebuhr, J. (1997). Identification of an ATPase activity associated with a 71-kilodalton polypeptide encoded in gene 1 of the human coronavirus 229E. *J. Virol.* **71,** 5631–5634.

Jiang, P., Chen, P. Y., Dong, Y. Y., Cai, J. L., Cai, B. X., and Jiang, Z. H. (2000). Isolation and genome characterization of porcine reproductive and respiratory syndrome virus in P.R. China. *J. Vet. Diagn. Invest.* **12,** 156–158.

Kadare, G., David, C., and Haenni, A. L. (1996). ATPase, GTPase, and RNA binding activities associated with the 206-kilodalton protein of turnip yellow mosaic virus. *J. Virol.* **70,** 8169–8174.

Kadare, G., and Haenni, A. L. (1997). Virus-encoded RNA helicases. *J. Virol.* **71,** 2583–2590.

Kim, H. S., Kwang, J., Yoon, I. J., Joo, H. S., and Frey, M. L. (1993). Enhanced replication of porcine reproductive and respiratory syndrome (Prrs) virus in a homogeneous subpopulation of Ma-104 cell line. *Arch. Virol.* **133,** 477–483.

Li, H., Clum, S., You, S., Ebner, K. E., and Padmanabhan, R. (1999). The serine protease and RNA-stimulated nucleoside triphosphatase and RNA helicase functional domains of dengue virus type 2 NS3 converge within a region of 20 amino acids. *J. Virol.* **73,** 3108–3116.

McElroy, W. D., and DeLuca, M. A. (1983). Firefly and bacterial luminescence: Basic science and applications. *J. Appl. Biochem.* **5,** 197–209.

Meulenberg, J. J., Hulst, M. M., de Meijer, E. J., Moonen, P. L., den Besten, A., de Kluyver, E. P., Wensvoort, G., and Moormann, R. J. (1993). Lelystad virus, the causative agent of porcine epidemic abortion and respiratory syndrome (PEARS), is related to LDV and EAV. *Virology* **192,** 62–72.

Meulenberg, J. J., Bos-de Ruijter, J. N., van de Graaf, R., Wensvoort, G., and Moormann, R. J. (1998). Infectious transcripts from cloned genome-length cDNA of porcine reproductive and respiratory syndrome virus. *J. Virol.* **72,** 380–387.

Motulski, H. J. (1999). "Analyzing Data with GraphPad Prism." GraphPad Software Inc., San Diego, CA.

Moyer, J. D., and Henderson, J. F. (1983). Nucleoside triphosphate specificity of firefly luciferase. *Anal. Biochem.* **131,** 187–189.

Murtaugh, M. P., Elam, M. R., and Kakach, L. T. (1995). Comparison of the structural protein coding sequences of the VR-2332 and Lelystad virus strains of the PRRS virus. *Arch. Virol.* **140,** 1451–1460.

Murtaugh, M. P., Faaberg, K. S., Laber, J., Elam, M., and Kapur, V. (1998). Genetic variation in the PRRS virus. *Adv. Exp. Med. Biol.* **440,** 787–794.

Nelsen, C. J., Murtaugh, M. P., and Faaberg, K. S. (1999). Porcine reproductive and respiratory syndrome virus comparison: Divergent evolution on two continents. *J. Virol.* **73,** 270–280.

Nielsen, H. S., Storgaard, T., and Oleksiewicz, M. B. (2000). Analysis of ORF 1 in European porcine reproductive and respiratory syndrome virus by long RT-PCR and restriction fragment length polymorphism (RFLP) analysis. *Vet. Microbiol.* **76,** 221–228.

Plagemann, P. G., and Moennig, V. (1992). Lactate dehydrogenase-elevating virus, equine arteritis virus, and simian hemorrhagic fever virus: A new group of positive-strand RNA viruses. *Adv. Virus Res.* **41,** 99–192.

Preugschat, F., Averett, D. R., Clarke, B. E., and Porter, D. J. (1996). A steady-state and pre-steady-state kinetic analysis of the NTPase activity associated with the hepatitis C virus NS3 helicase domain. *J. Biol. Chem.* **271,** 24449–24457.

Rikkonen, M., Peranen, J., and Kaariainen, L. (1994). ATPase and GTPase activities associated with Semliki Forest virus nonstructural protein nsP2. *J. Virol.* **68,** 5804–5810.

Sambrook, J. (1989). "Molecular Cloning. A Laboratory Manual." 2nd ed., Cold Spring Harbor Laboratory Press, Plainview, NY.

Seybert, A., van Dinten, L. C., Snijder, E. J., and Ziebuhr, J. (2000a). Biochemical characterization of the equine arteritis virus helicase suggests a close functional relationship between arterivirus and coronavirus helicases. *J. Virol.* **74,** 9586–9593.

Seybert, A., Hegyi, A., Siddell, S. G., and Ziebuhr, J. (2000b). The human coronavirus 229E superfamily 1 helicase has RNA and DNA duplex-unwinding activities with 5′-to-3′ polarity. *RNA* **6,** 1056–1068.

Shen, S., Kwang, J., Liu, W., and Liu, D. X. (2000). Determination of the complete nucleotide sequence of a vaccine strain of porcine reproductive and respiratory syndrome virus and identification of the Nsp2 gene with a unique insertion. *Arch. Virol.* **145,** 871–883.

Smith, P. K., Krohn, R. I., Hermanson, G. T., Mallia, A. K., Gartner, F. H., Provenzano, M. D., Fujimoto, E. K., Goeke, N. M., Olson, B. J., and Klenk, D. C. (1985). Measurement of protein using bicinchoninic acid. *Anal. Biochem.* **150,** 76–85.

Snijder, E. J., Wassenaar, A. L., and Spaan, W. J. (1992). The 5′ end of the equine arteritis virus replicase gene encodes a papainlike cysteine protease. *J. Virol.* **66,** 7040–7048.

Snijder, E. J., Wassenaar, A. L., and Spaan, W. J. (1993a). Proteolytic processing of the N-terminal region of the equine arteritis virus replicase. *Adv. Exp. Med. Biol.* **342,** 227–732.

Snijder, E. J., Horzinek, M. C., and Spaan, W. J. (1993b). The coronaviruslike superfamily. *Adv. Exp. Med. Biol.* **342,** 235–244.

Snijder, E. J., Wassenaar, A. L., and Spaan, W. J. (1994). Proteolytic processing of the replicase ORF1a protein of equine arteritis virus. *J. Virol.* **68,** 5755–5764.

Snijder, E. J., Wassenaar, A. L., Spaan, W. J., and Gorbalenya, A. E. (1995). The arterivirus Nsp2 protease. An unusual cysteine protease with primary structure similarities to both papain-like and chymotrypsin-like proteases. *J. Biol. Chem.* **270,** 16671–16676.

Snijder, E. J., Wassenaar, A. L., van Dinten, L. C., Spaan, W. J., and Gorbalenya, A. E. (1996). The arterivirus nsp4 protease is the prototype of a novel group of chymotrypsin-like enzymes, the 3C-like serine proteases. *J. Biol. Chem.* **271,** 4864–4871.

Snijder, E. J. (1998). The arterivirus replicase. The road from RNA to protein(s), and back again. *Adv. Exp. Med. Biol.* **440,** 97–108.

Snijder, E. J., and Meulenberg, J. J. M. (1998). The molecular biology of arteriviruses. *J. Gen. Virol.* **79,** 961–979.

Tamura, J. K., Warrener, P., and Collett, M. S. (1993). RNA-stimulated NTPase associated with the P80 protein of the pestivirus bovine viral diarrhea virus. *Virology* **193,** 1–10.

van Dinten, L. C., Wassenaar, A. L., Gorbalenya, A. E., Spaan, W. J., and Snijder, E. J. (1996). Processing of the equine arteritis virus replicase ORF1b protein: Identification of cleavage products containing the putative viral polymerase and helicase domains. *J. Virol.* **70,** 6625–6633.

van Dinten, L. C., den Boon, J. A., Wassenaar, A. L., Spaan, W. J., and Snijder, E. J. (1997). An infectious arterivirus cDNA clone: Identification of a replicase point mutation that abolishes discontinuous mRNA transcription. *Proc. Natl. Acad. Sci. USA* **94,** 991–996.

van Dinten, L. C., Rensen, S., Gorbalenya, A. E., and Snijder, E. J. (1999). Proteolytic processing of the open reading frame 1b-encoded part of arterivirus replicase is mediated by nsp4 serine protease and is essential for virus replication. *J. Virol.* **73,** 2027–2037.

van Dinten, L. C., van Tol, H., Gorbalenya, A. E., and Snijder, E. J. (2000). The predicted metal-binding region of the arterivirus helicase protein is involved in subgenomic mRNA synthesis, genome replication, and virion biogenesis. *J. Virol.* **74,** 5213–5223.

van Marle, G., van Dinten, L. C., Spaan, W. J., Luytjes, W., and Snijder, E. J. (1999). Characterization of an equine arteritis virus replicase mutant defective in subgenomic mRNA synthesis. *J. Virol.* **73,** 5274–5281.

Wassenaar, A. L., Spaan, W. J., Gorbalenya, A. E., and Snijder, E. J. (1997). Alternative proteolytic processing of the arterivirus replicase ORF1a polyprotein: Evidence that NSP2 acts as a cofactor for the NSP4 serine protease. *J. Virol.* **71,** 9313–9322.

Wootton, S., Yoo, D., and Rogan, D. (2000). Full-length sequence of a Canadian porcine reproductive and respiratory syndrome virus (PRRSV) isolate. *Arch. Virol.* **145,** 2297–2323.

Yuan, S., Nelsen, C. J., Murtaugh, M. P., Schmitt, B. J., and Faaberg, K. S. (1999). Recombination between North American strains of porcine reproductive and respiratory syndrome virus. *Virus Res.* **61,** 87–98.

Yuan, S., Mickelson, D., Murtaugh, M. P., and Faaberg, K. S. (2001). Complete genome comparison of porcine reproductive and respiratory syndrome virus parental and attenuated strains. *Virus Res.* **74,** 99–110.

Ziebuhr, J., Snijder, E. J., and Gorbalenya, A. E. (2000). Virus-encoded proteinases and proteolytic processing in the Nidovirales. *J. Gen. Virol.* **4,** 853–879.